

**Supplemental Information**

**Gold nanoparticles decorated with ovalbumin-  
derived epitopes: effect of shape and size on T-cell  
immune responses**

*Elena A. Egorova,<sup>a</sup> Gerda E.M. Lamers,<sup>b</sup> Fazel Abdolahpur Monikh,<sup>c</sup> Aimee L. Boyle,<sup>d</sup>  
Bram Slütter,<sup>e</sup> Alexander Kros<sup>\*a</sup>*

<sup>a</sup> Department of Supramolecular & Biomaterials Chemistry, Leiden Institute of Chemistry,  
Leiden University, The Netherlands

<sup>b</sup> Core Facility Microscopy, Institute of Biology, Leiden University, the Netherlands

<sup>c</sup> Environmental Biology, Institute of Environmental Sciences, Leiden University, The  
Netherlands

<sup>d</sup> Macromolecular Biochemistry, Leiden Institute of Chemistry, Leiden University, The  
Netherlands

<sup>e</sup> Leiden Academic Centre for Drug Research, Biotherapeutics, Leiden University, The  
Netherlands

## Table of content

<b>Figure S1.</b> Sample characterization before and after modification obtained with DLS.....	3
<b>Figure S2.</b> GNP and GNR characteristics determined with ICP-MS.....	4
<b>Scheme S1.</b> Chemical structure of <b>W</b> .....	4
<b>Figure S3.</b> GNP and GNR cytotoxicity evaluated with an LDH release assay.....	5
<b>Figure S4 (A,B).</b> TEM micrographs of cell sections.....	6
<b>Figure S4 (C,D).</b> TEM micrographs of cell sections.....	7
<b>Figure S4 (E,F).</b> TEM micrographs of cell sections.....	8
<b>Figure S4 (G).</b> TEM micrographs of cell sections.....	9
<b>Figure S5.</b> TEM analysis of vesicles found in BMDC sections.....	9
<b>Figure S6.</b> Flow cytometry gating strategy for OT-I and OT-II experiments.....	10
<b>Figure S7.</b> Gating strategy used in flow cytometry analysis of antigen processing and presentation by BMDCs.....	11
<b>Figure S8.</b> Detection of MHC-I/OVA <sub>257-264</sub> complex on the cell surface.....	12
<b>Figure S9.</b> Detection of MHC-I/OVA <sub>257-264</sub> complex on the cell surface (controls).....	13
<b>Figure S10.</b> IL-12 levels induced by treatment with GNPs and GNRs.....	13
<b>Figure S11.</b> IL-12 levels induced by treatment with control substances.....	14
<b>Figure S12.</b> IL-1 $\beta$ levels induced by treatment with GNPs and GNRs.....	14
<b>Figure S13.</b> Flow cytometry gating strategy for the BMDCs activation study.....	15
<b>Figure S14.</b> Upregulation profiles for CD80 cellular marker.....	16
<b>Figure S15.</b> Upregulation profiles for CD86 cellular marker.....	17
<b>Figure S16.</b> Upregulation profiles for CD80 cellular marker (controls).....	18
<b>Figure S17.</b> Upregulation profiles for CD86 cellular marker (controls).....	19
<b>Figure S18.</b> LC-MS spectrum for <b>base</b> .....	20
<b>Figure S19.</b> LC-MS spectrum for <b>1</b> .....	20
<b>Figure S20.</b> LC-MS spectrum for OVA <sub>257-264</sub> .....	21
<b>Figure S21.</b> LC-MS spectrum for <b>2</b> .....	21
<b>Figure S22.</b> LC-MS spectrum for OVA <sub>323-339</sub> .....	22
<b>Figure S23.</b> LC-MS spectrum for <b>W</b> .....	22

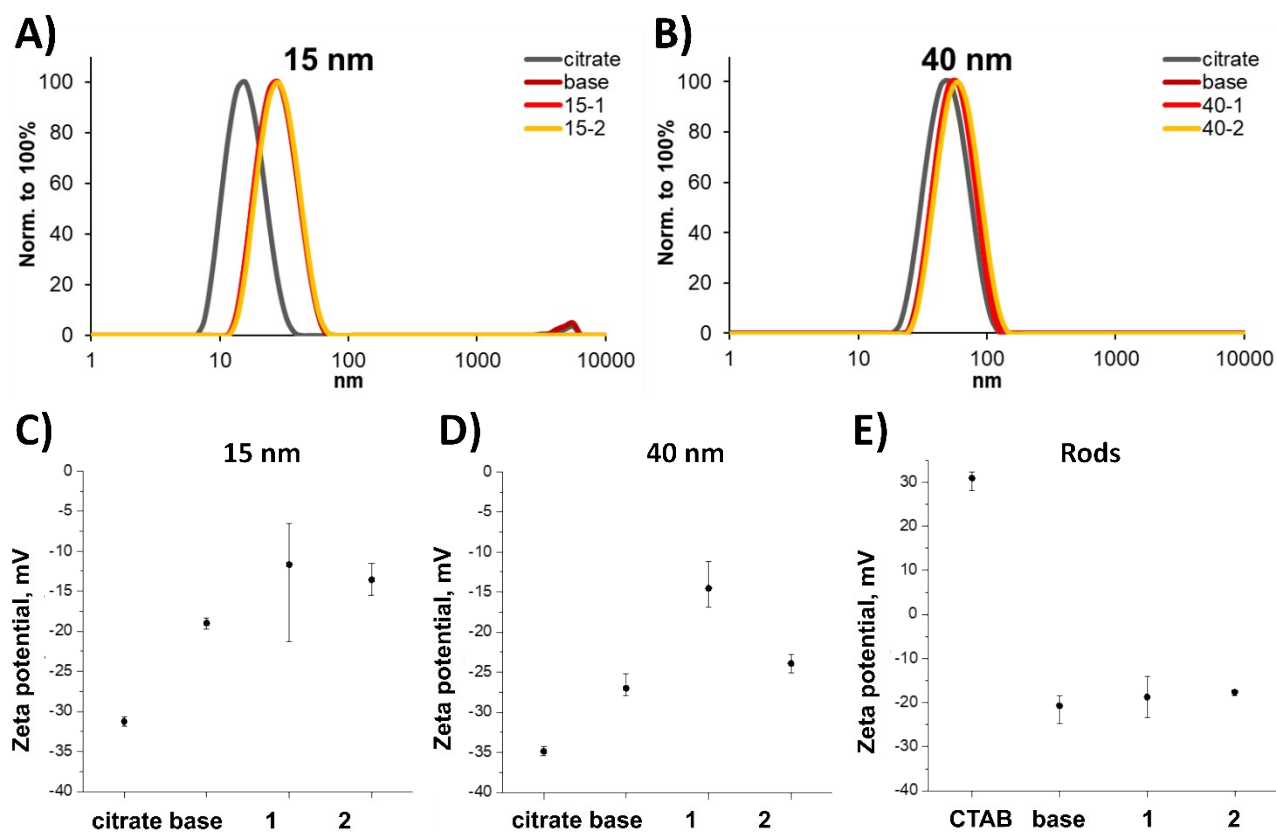


**Figure S1.** Sample characterization before and after modification obtained with DLS: (A) size distribution for 15 nm GNPs; (B) size distribution for 40 nm GNPs; (C) zeta potential values for 15 nm GNPs; (D) zeta potential values for 40 nm GNPs; (E) zeta potential values for GNRs. (A, B) samples were prepared in PBS (pH 7.2); (C-E) samples were prepared in PBS (pH 7.2) and diluted 10 times with MilliQ prior the measurement. Zeta potential is shown as a mean of three measurements with error bars indicating max and min values. Due to their shape, GNRs could not be analyzed for their hydrodynamic diameter.

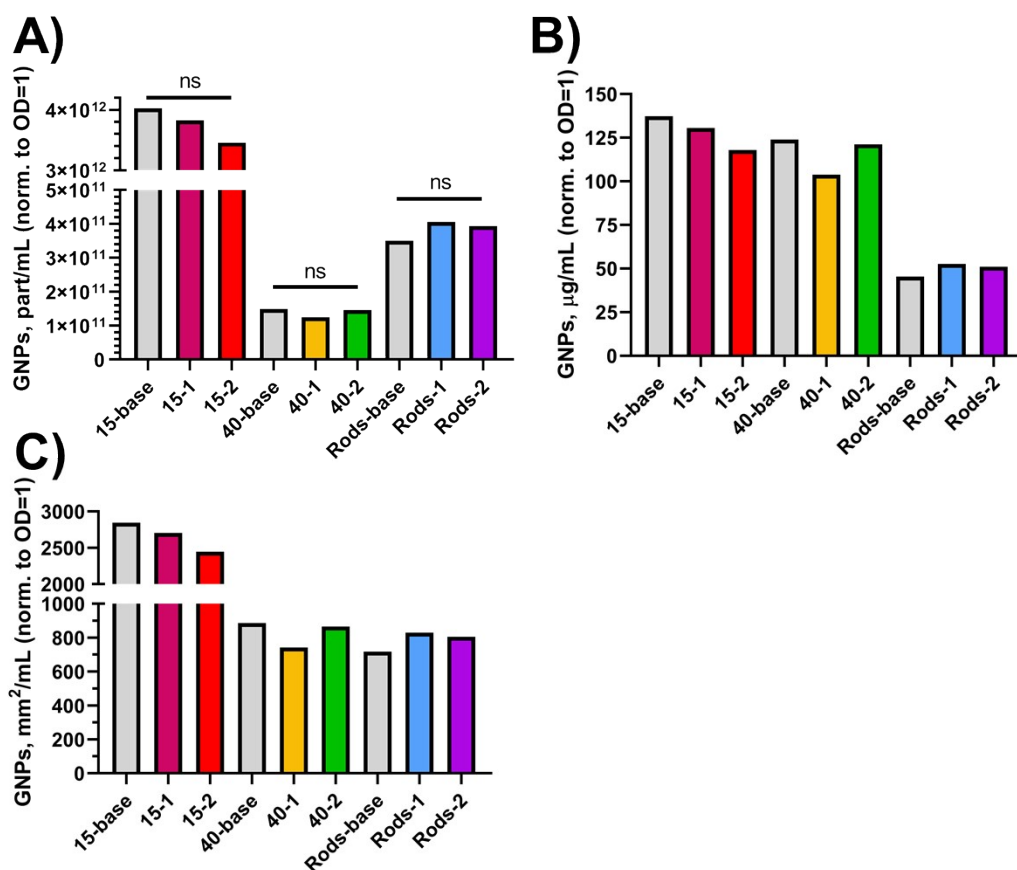
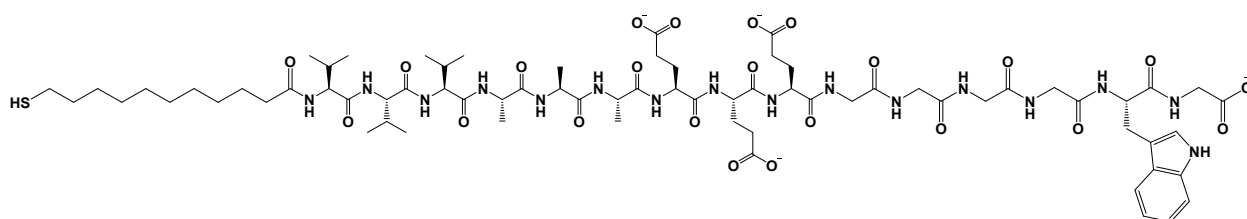


**Figure S2.** GNP and GNR characteristics determined with ICP-MS and normalized to a suspension with an optical density of 1 ( $OD_{LSPR} = 1$ ): (A) number concentration; (B) mass concentration; and (C) total gold surface available for contact as a function of volume. The mass concentration was measured once. To determine the significance of the difference between the concentrations of particles with the same gold core but different coating, a 10% deviation was introduced. According to a two-way ANOVA test performed in GraphPad Prism software, differences in metrics of nanoparticles comprising the same gold core, were found to be non-significant (ns). Mass of one nanoparticle in ag: 15 nm GNPs = 34.1; 40 nm GNPs = 832.2; GNRs = 129.8. Surface area of one nanoparticle in nm<sup>2</sup>: 15 nm GNPs = 706.86; 40 nm GNPs = 5944.7; GNRs = 2045.8.



**Scheme S1.** Chemical structure of **W** used to determine the coverage density and antigen loading onto different GNPs and GNRs.

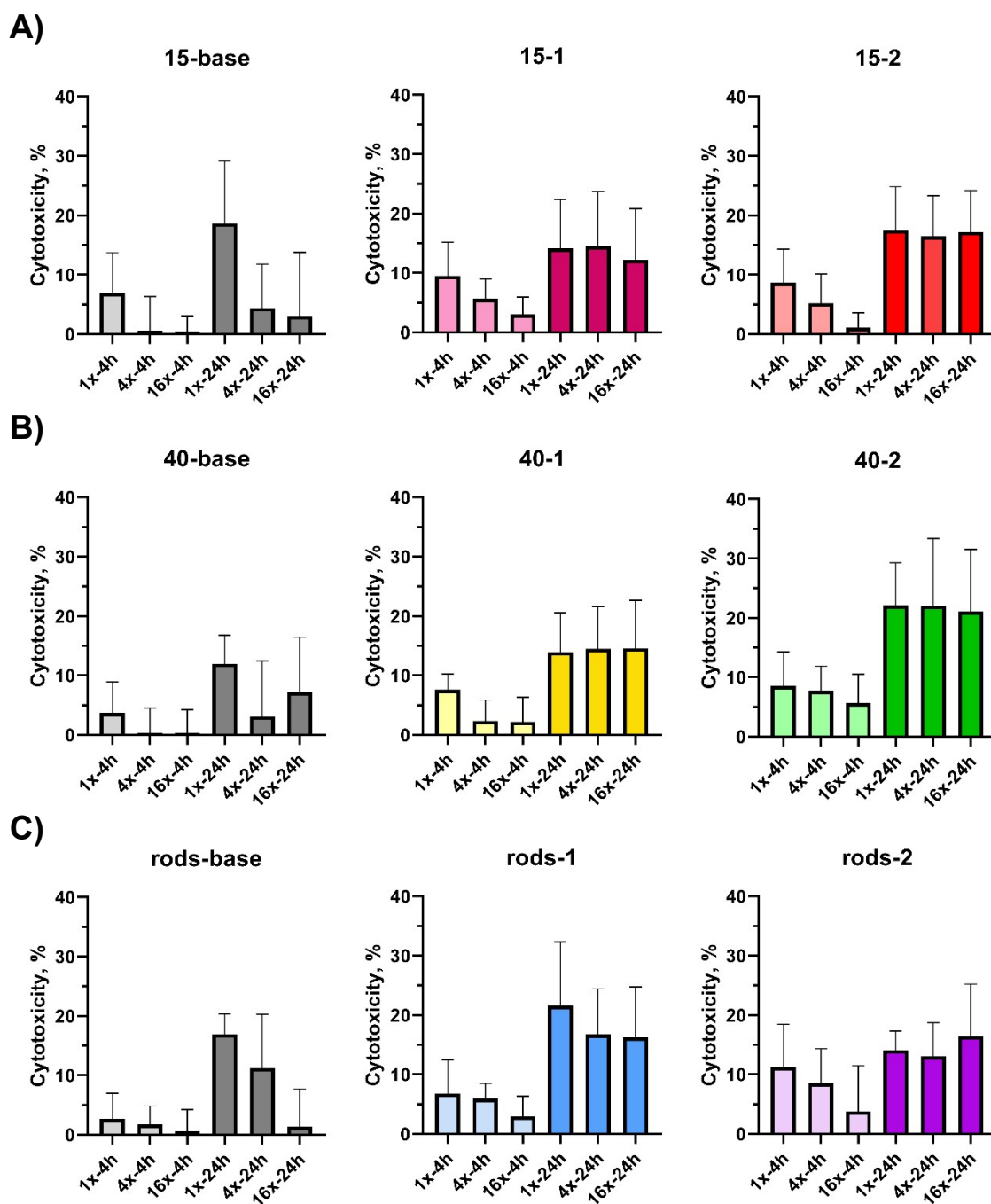


**Figure S3.** Cytotoxicity evaluated with an LDH release assay for: (panel A) 15 nm GNPs, (panel B) 40 nm GNPs, and (panel C) GNRs. GNP concentration range analyzed involved 1x, 4x, and 16x times diluted samples (Table S2). Lighter color shades indicate 4 h exposure time; darker shades – 24 h exposure time. Error bars indicate standard deviations and were calculated using GraphPad Prism software.

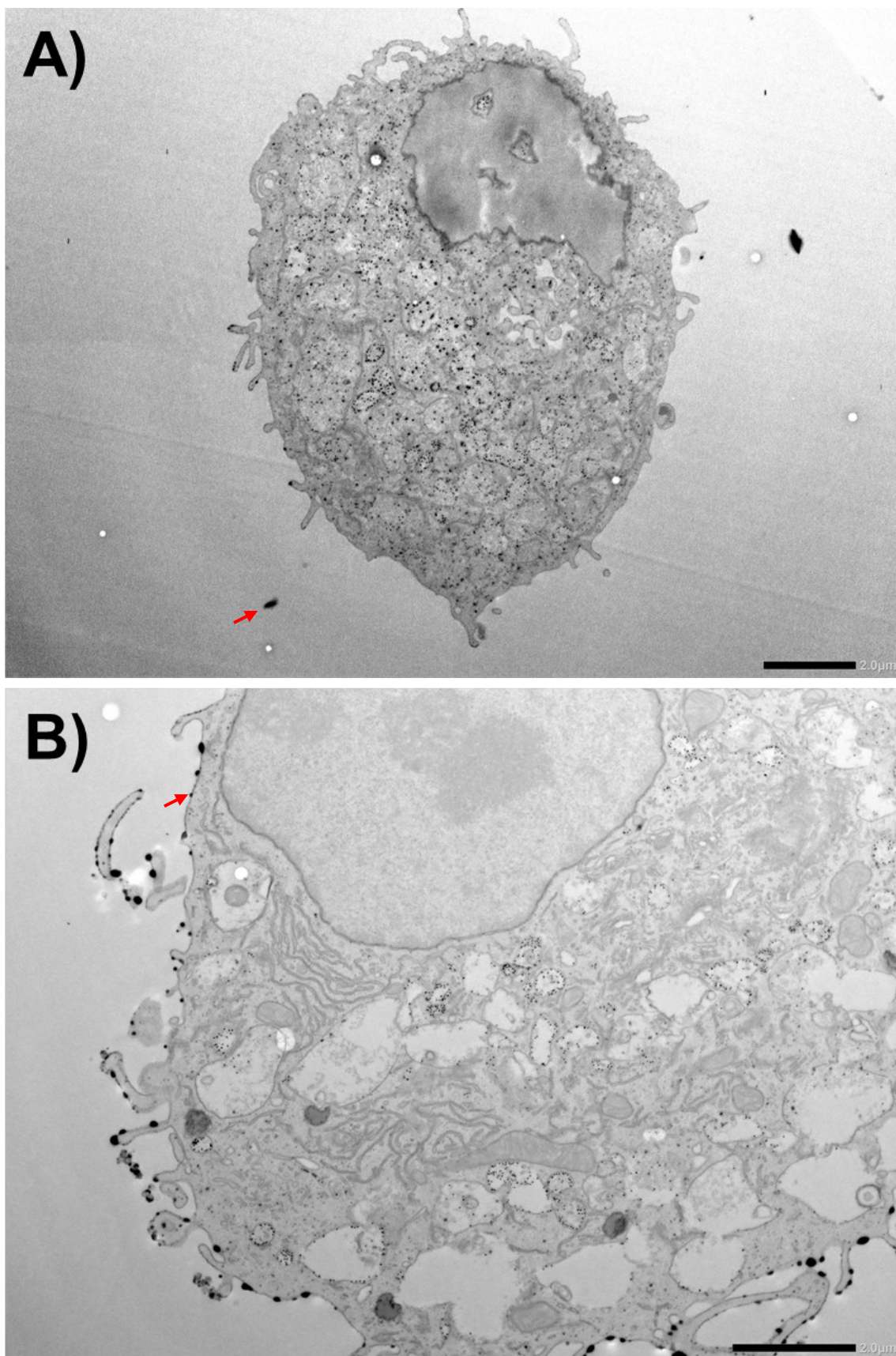


**Figure S4 (A,B).** TEM micrographs of cell sections: (A) BMDCs exposed to **15-1** and (B) BMDCs exposed to **15-2**. Scale bars = 2 μm. The round dark crystals on the outer side of the cell membrane are accumulations of the  $\text{OsO}_4$  staining (indicated by arrows).



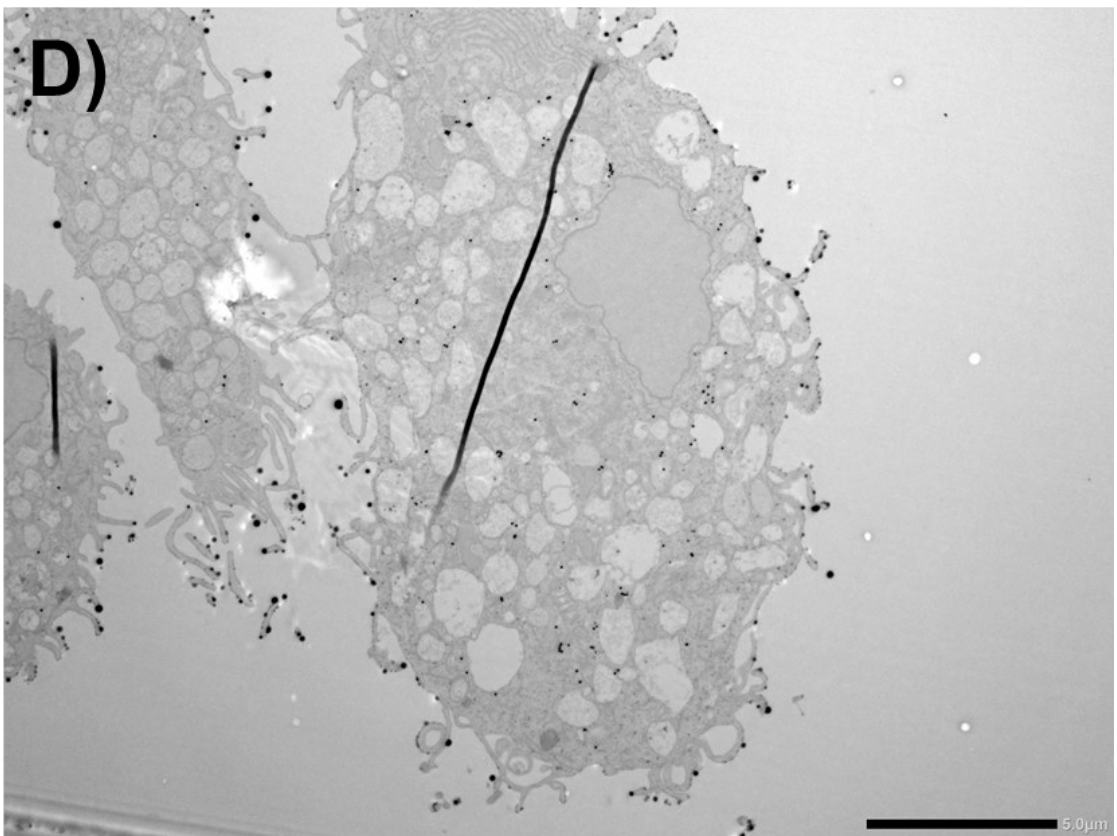
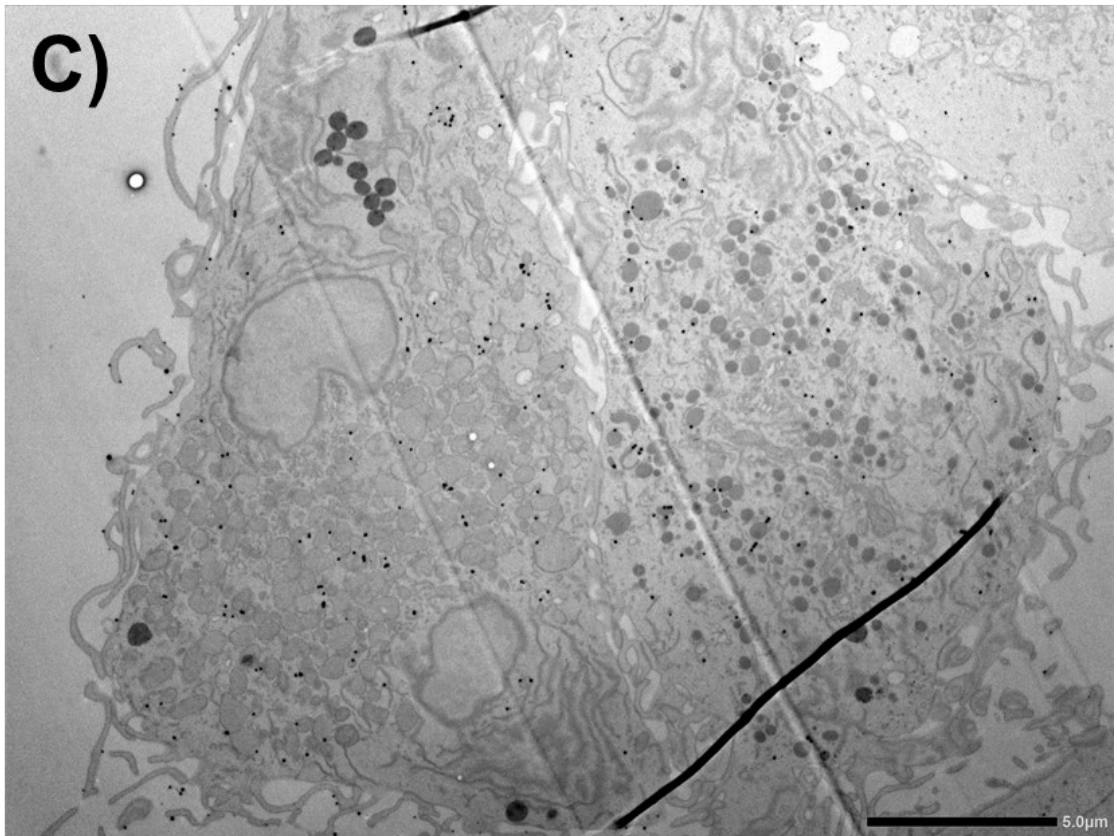


**Figure S4 (C,D).** TEM micrographs of cell sections: (C) BMDCs exposed to **40-1** and (D) BMDCs exposed to **40-2**. Scale bars = 5  $\mu$ m. The round dark crystals on the outer side of the cell membrane are the accumulations of the  $\text{OsO}_4$  staining.

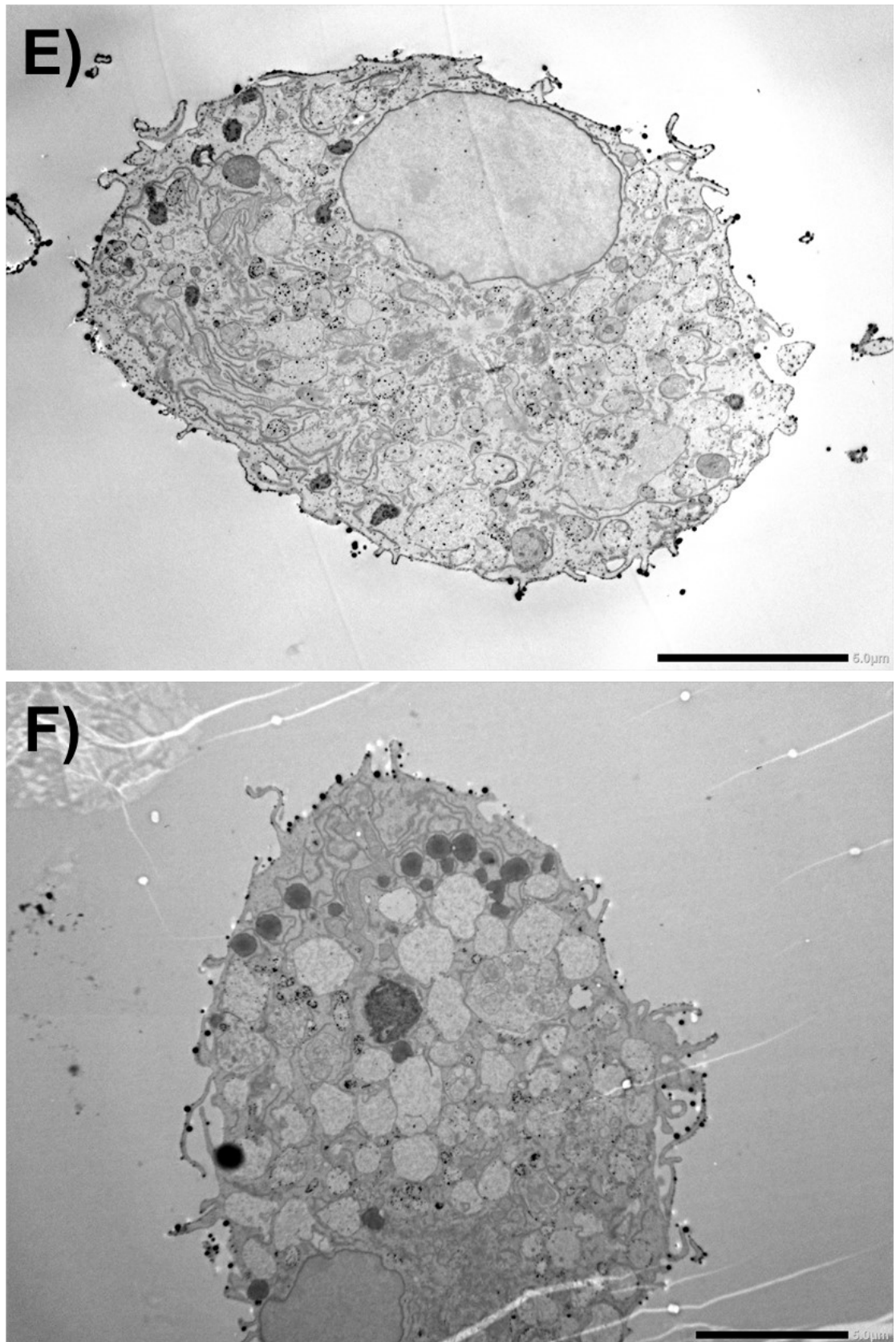


**Figure S4 (E,F).** TEM micrographs of cell sections: (E) BMDCs exposed to **Rods-1** and (F) DBMCs exposed to **Rods-2**. Scale bars = 5  $\mu\text{m}$ . The round dark crystals on the outer side of the cell membrane are the accumulations of the  $\text{OsO}_4$  staining.



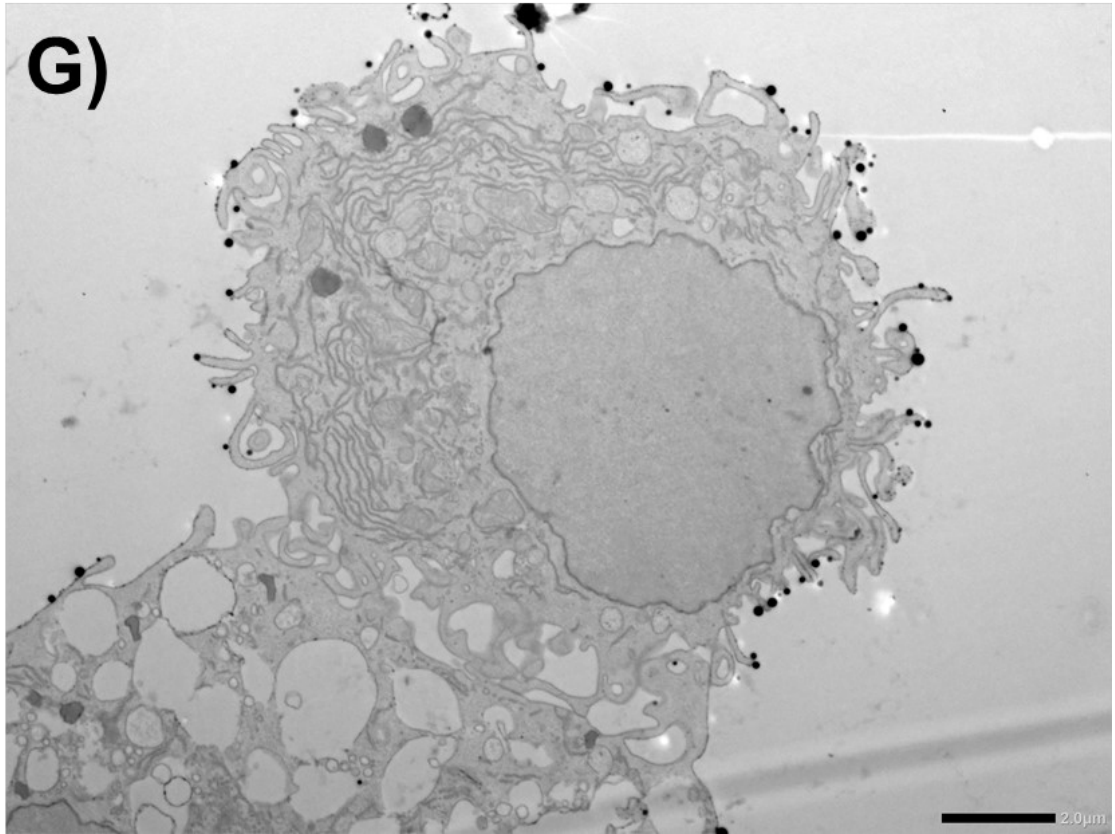


**Figure S4 (G).** TEM micrograph of a cell section: (G) BMDCs treated with PBS. Scale bars = 2  $\mu$ m. The round dark crystals on the outer side of cell membrane are the accumulations of the OsO<sub>4</sub> staining.

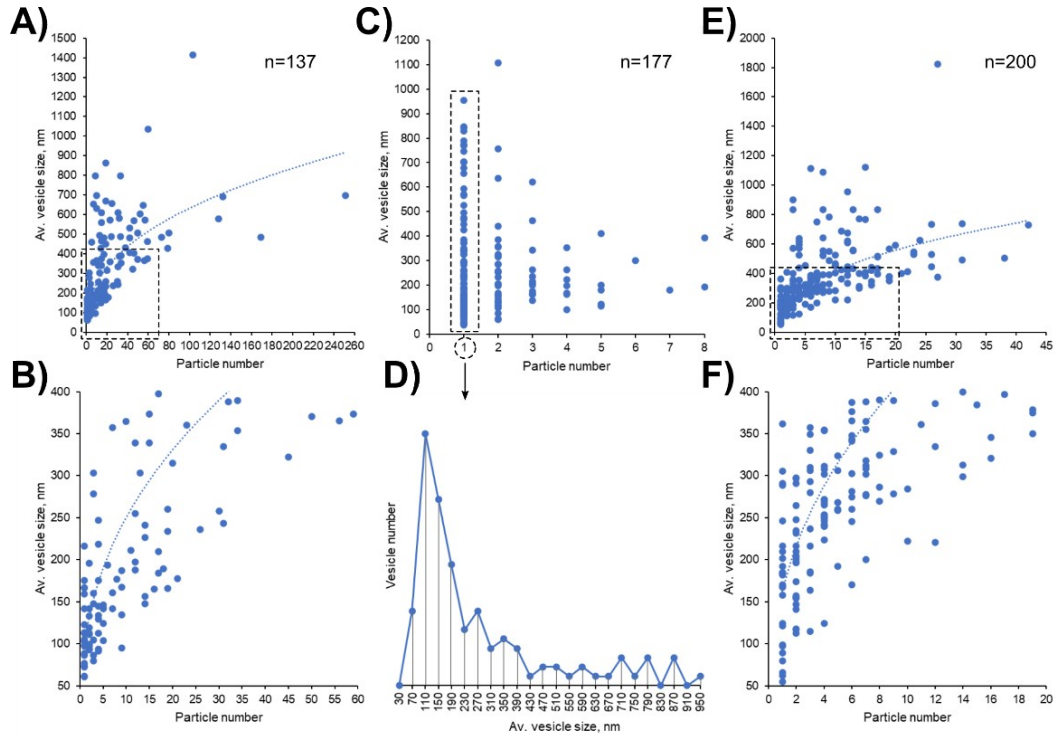


**Figure S5.** Quantitative analysis of the TEM images of BMDC sections was done on the basis of average vesicle size and number of entrapped nanoparticles: (A-B) **15-1**, (C-D) **40-1**, and (E) **Rods-1**. Depending on the vesicle type, they were hypothesized to be different stages of endosomes, lysosomes, autophagosomes *etc* (in order of increasing size). For example, (D) shows the size distribution of vesicles with 1 entrapped particle of **40-1**. These were suspected to be endocytic vesicles (40-120 nm). Autophagosomes are large vesicles (> 1000 nm) filled with smaller vesicles. Lysosomes are typically large and vary in size.

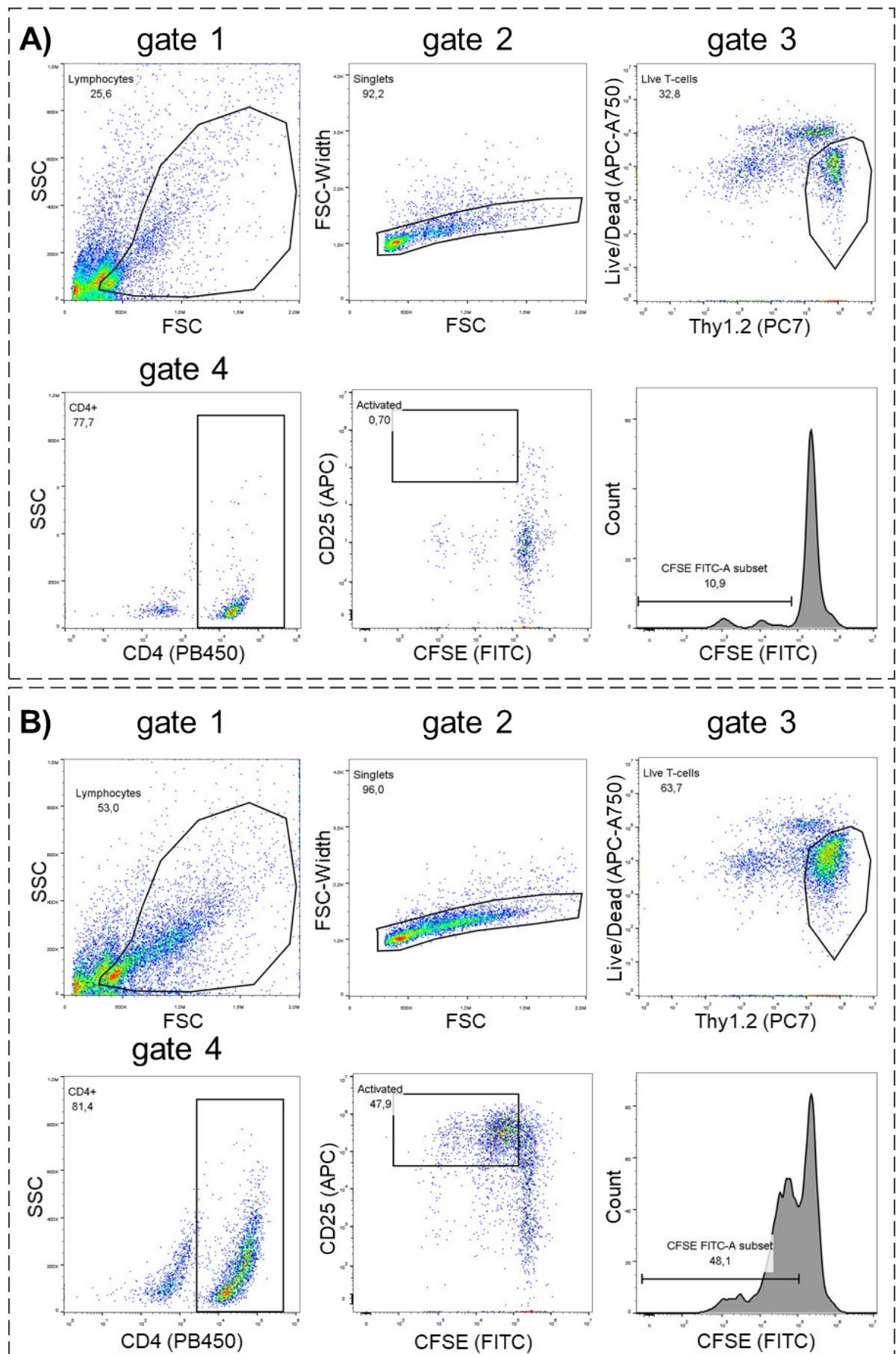


**Figure S6.** Flow cytometry gating strategy for OT-I and OT-II mice *ex vivo* experiments: (panel A) negative control – PBS and (panel B) positive control – 20 ng/well OVA<sub>323-339</sub>. Data were analyzed on the area basis. Values for CD25<sup>+</sup> versus CFSE<sup>low</sup> are shown in **Figure 4**.

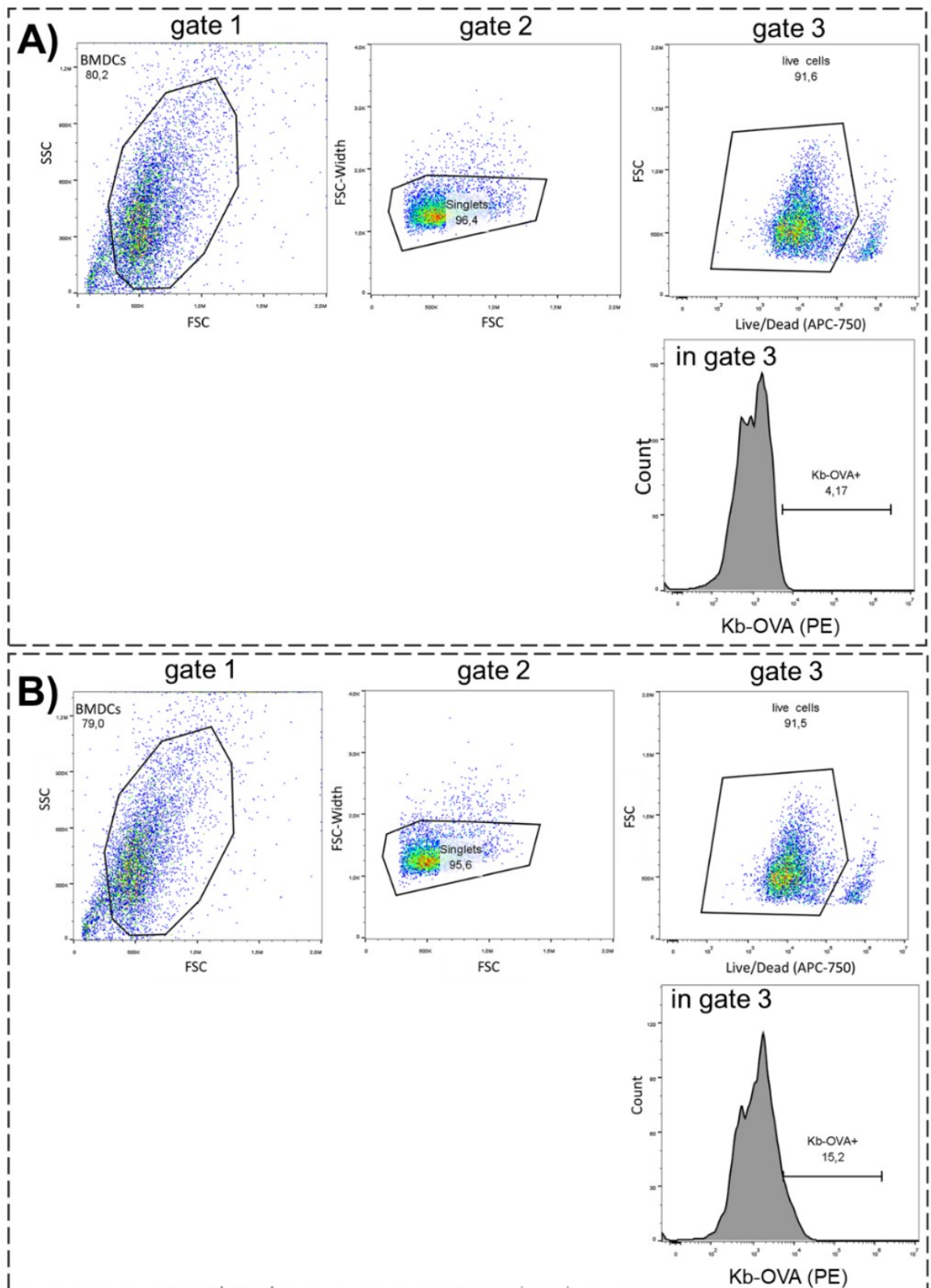


**Figure S7.** Gating strategy used in flow cytometry analysis of antigen processing and presentation by BMDCs upon exposure to epitope-decorated GNPs and GNRs. (panel A) negative control – DMEM medium and (panel B) positive control – 40 ng/well OVA<sub>257-264</sub>. Data were analyzed on the basis of area.

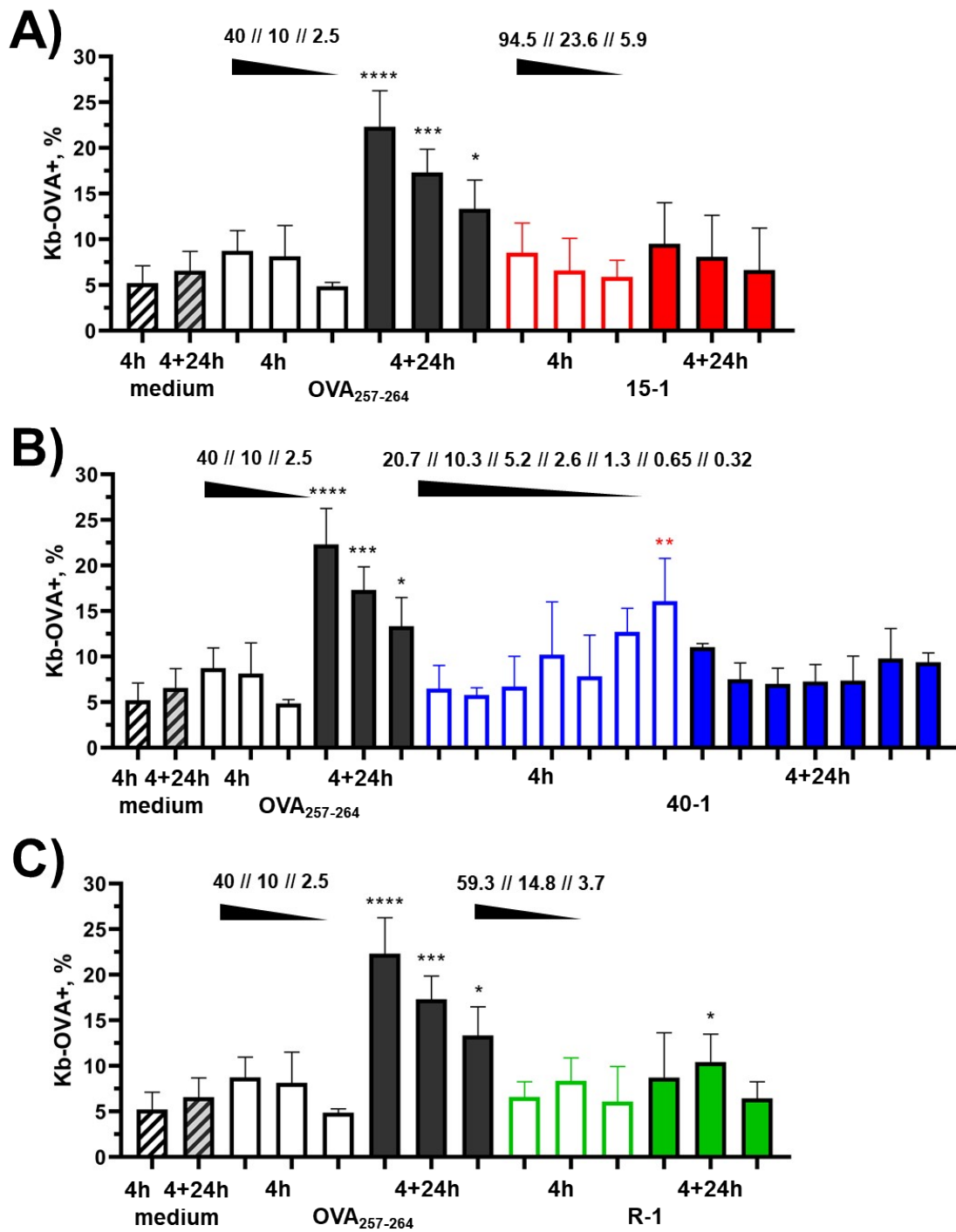


**Figure S8.** BMDCs activation was monitored through expression of the MHC-I/OVA<sub>257-264</sub> complex on the cell surface after a 4-hour incubation with GNPs and GNRs. The cell subset positive for this marker was compared to the negative control (medium) and positive control (OVA<sub>257-264</sub>): (A) **15-1**, (B) **40-1**, and (C) **R-1**. Empty columns show data right after the 4-hour incubation, and solid columns – after 24 hours incubation. Epitope dosage per well (in ng/well) is shown above the  $\blacktriangle$  indicator.



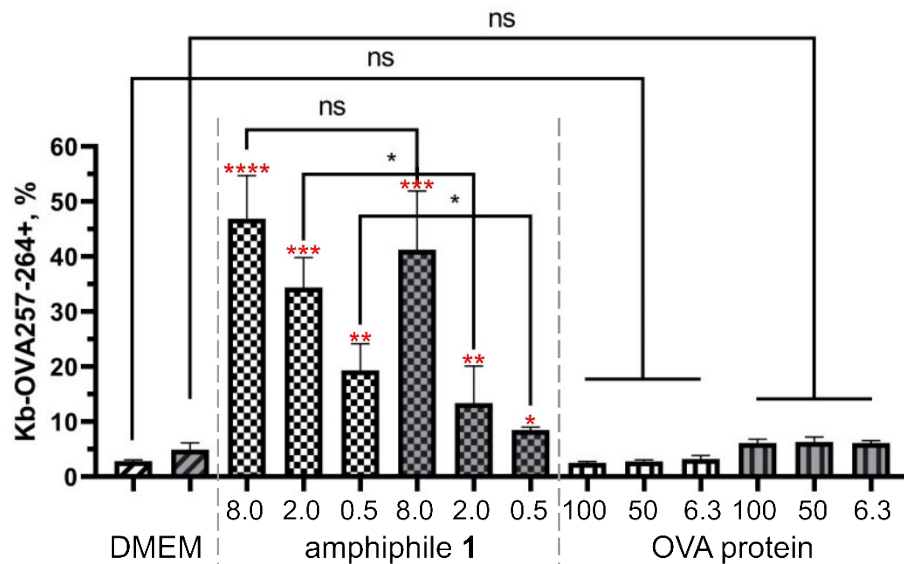


**Figure S9.** Upregulation of MHC-I/OVA<sub>257-264</sub> complex on the cell surface after a 4-hour incubation with control substances: amphiphile 1 and whole OVA protein. The cell subset positive for this marker was compared to the negative control (DMEM). Empty columns show data right after the 4-hour incubation, and solid with a gray fill – 24 hours after the incubation. Significance of amphiphile 1 in comparison to the negative control (DMEM) is shown in red. Dosage is given in µg/mL.

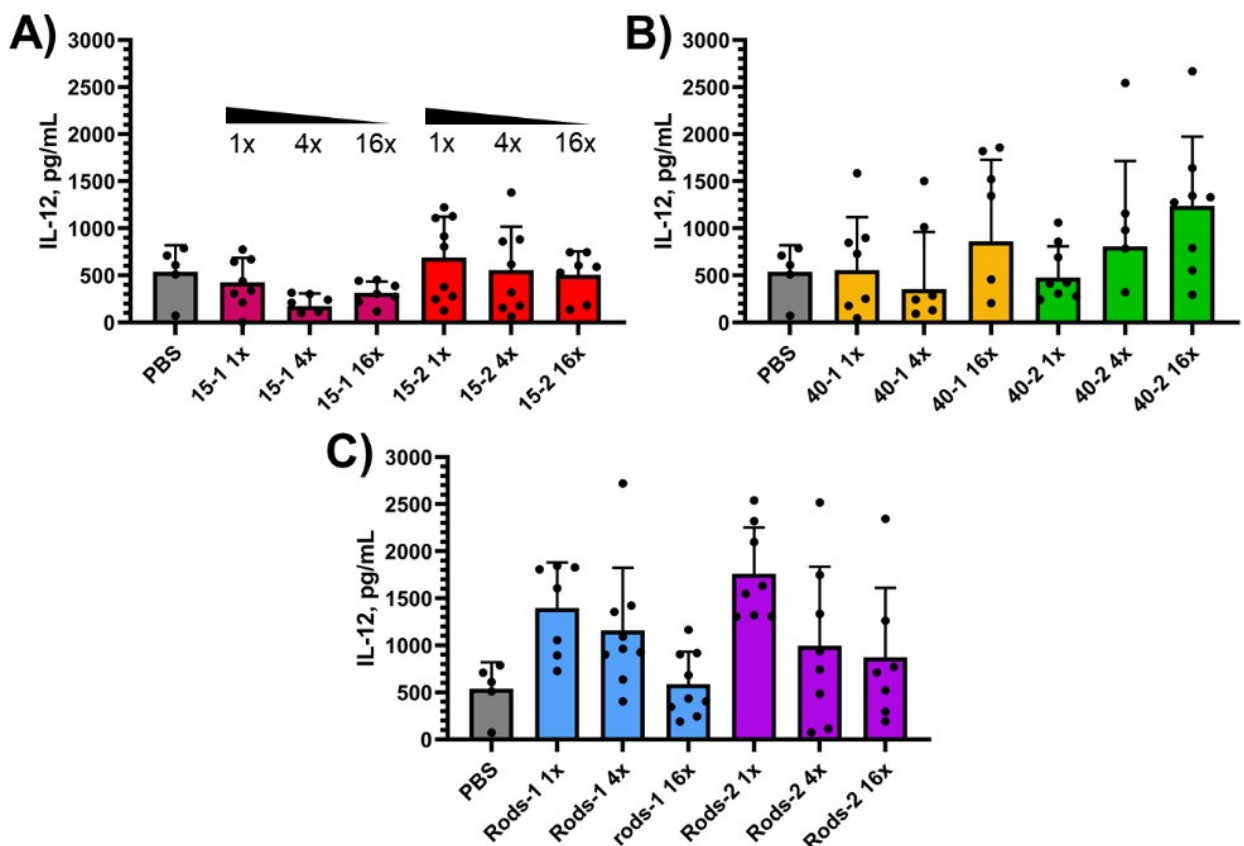


**Figure S10.** IL-12 levels in the cell culture supernatants of BMDCs after 24 h exposure to different GNPs: (A) GNPs with a 15 nm core; (B) GNPs with a 40 nm core; and (C) GNRs with a rod-like core of 45 by 15 nm in size. The BMDCs that were given PBS instead of GNPs or GNRs are present for comparison (gray color). The GNP concentration range analyzed included 1x, 4x, and 16x times diluted samples (Table S2). Error bars indicate standard deviations and were calculated using GraphPad Prism software.



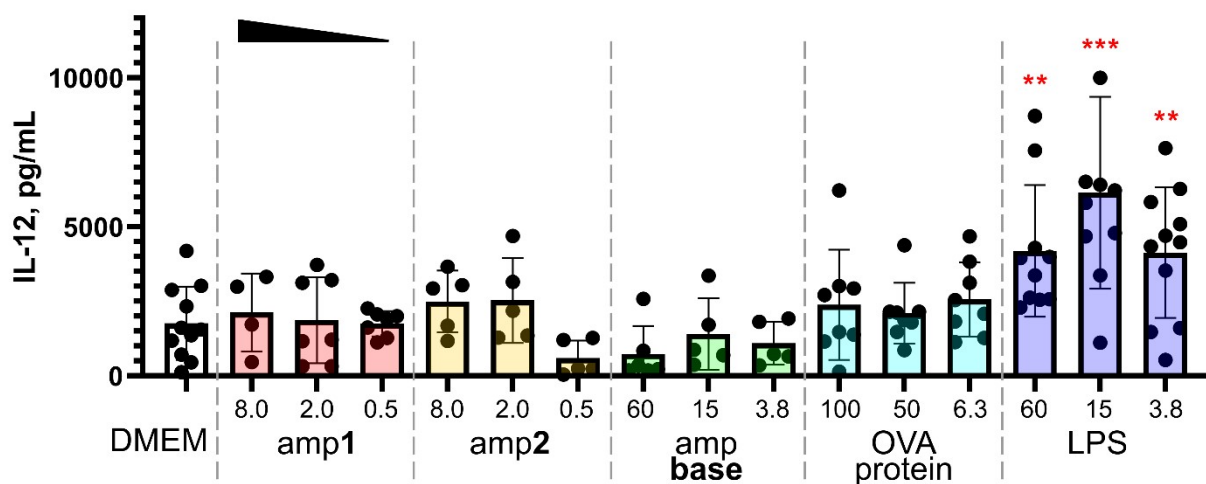


**Figure S11.** IL-12 levels in the cell culture supernatants of BMDCs after 24 h exposure to control substances: three peptide amphiphiles (amp1, amp2, amp base), whole ovalbumin protein (OVA protein), bacterial lipopolysaccharides (LPS). The dosage is comparable to that of the different GNPs. The concentrations are given in  $\mu\text{g/mL}$  of cell exposure medium. Only LPS samples showed statically significant difference compared to the DMEM control. Error bars indicate standard deviations and were calculated using GraphPad Prism software.

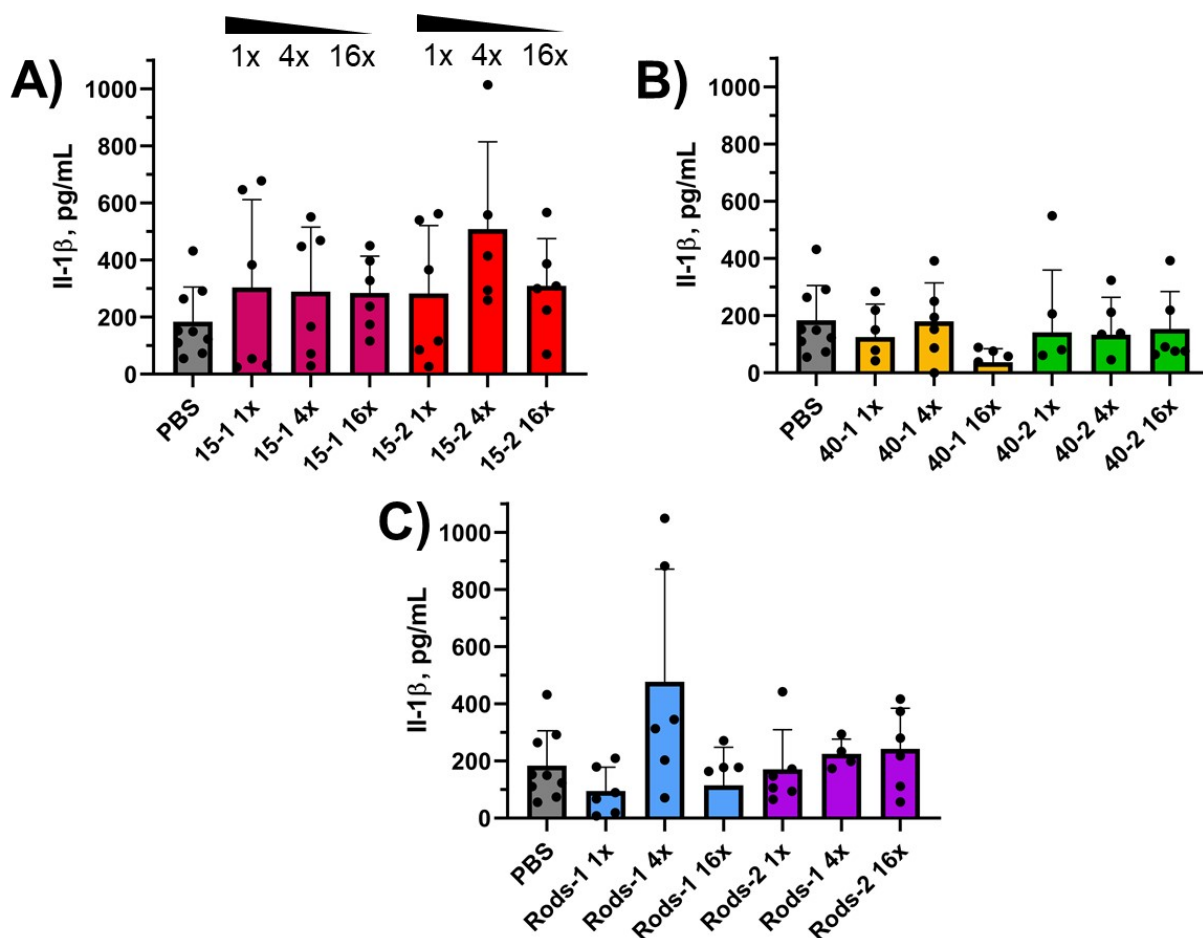


**Figure S12.** IL-1 $\beta$  levels in the cell culture supernatants of BMDCs after 24 h exposure to different GNPs: (A) GNPs with a 15 nm core; (B) GNPs with a 40 nm core; and (C) GNRs with a rod-like core of 45 by 15 nm in size. The BMDCs that were given PBS instead of GNPs or GNRs are present for comparison (gray color). GNP concentration range analyzed included 1x, 4x, and 16x times diluted samples (Table S2). Error bars indicate standard deviations and were calculated using GraphPad Prism software.



**Figure S13.** Gating strategy used in flow cytometry analysis of BMDCs activation by epitope-decorated GNPs and GNRs. (panel A) negative control – DMEM medium and (panel B) positive control – 40 ng/well OVA<sub>257-264</sub>. Data were analyzed on the basis of area.

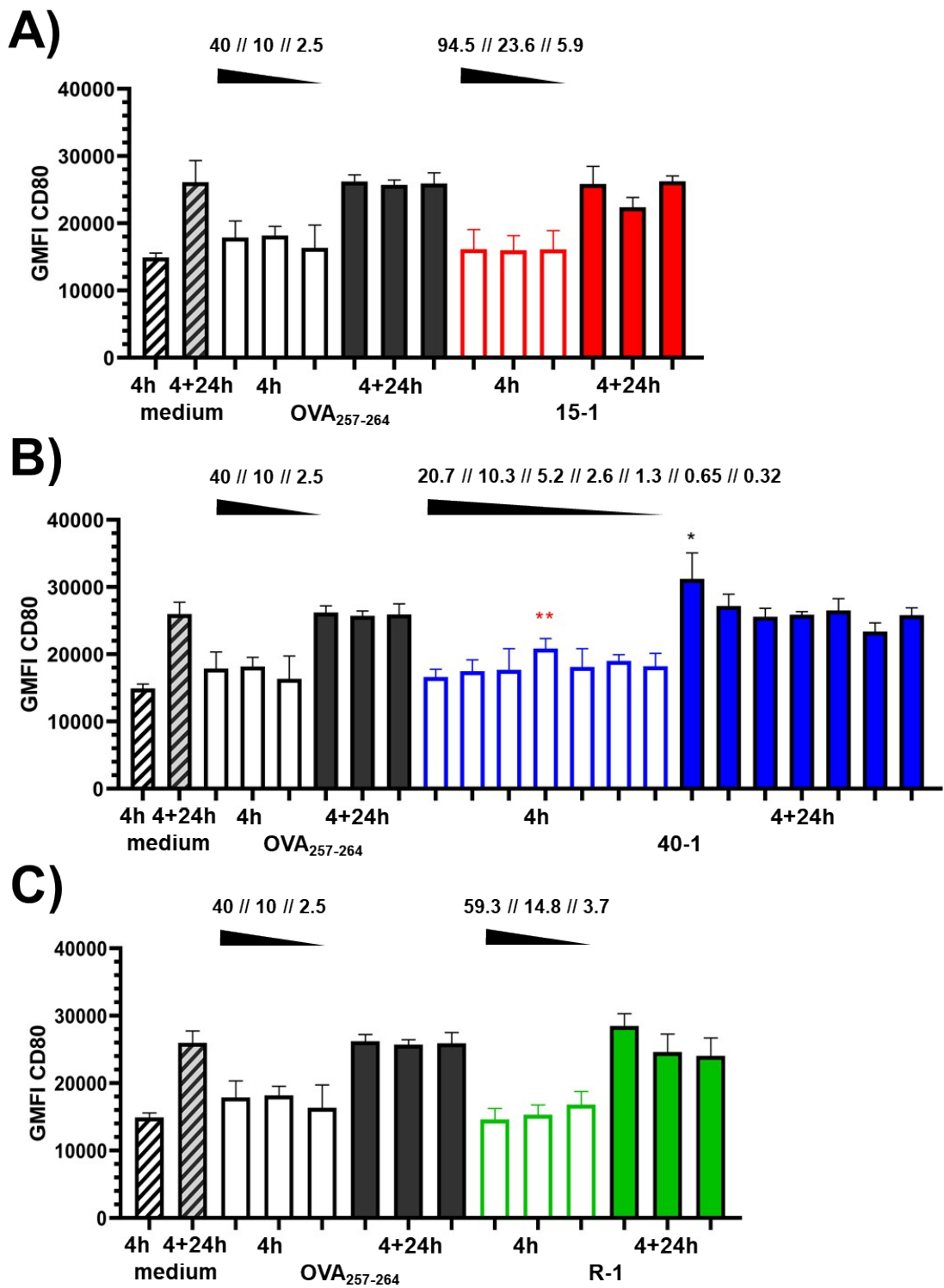


**Figure S14.** BMDCs activation was monitored through upregulation of CD80 cellular marker after a 4-hour incubation with GNPs and GNRs. Geometric mean fluorescence intensity (GMFI) gained for different samples was compared to the negative control (medium) and positive control (OVA<sub>257-264</sub>): (A) **15-1**, (B) **40-1**, and (C) **R-1**. Empty columns show data right after the 4-hour incubation, and solid columns – after 24 hours after the incubation. Epitope dosage per well (in ng/well) is shown above the  $\blacktriangle$  indicator.

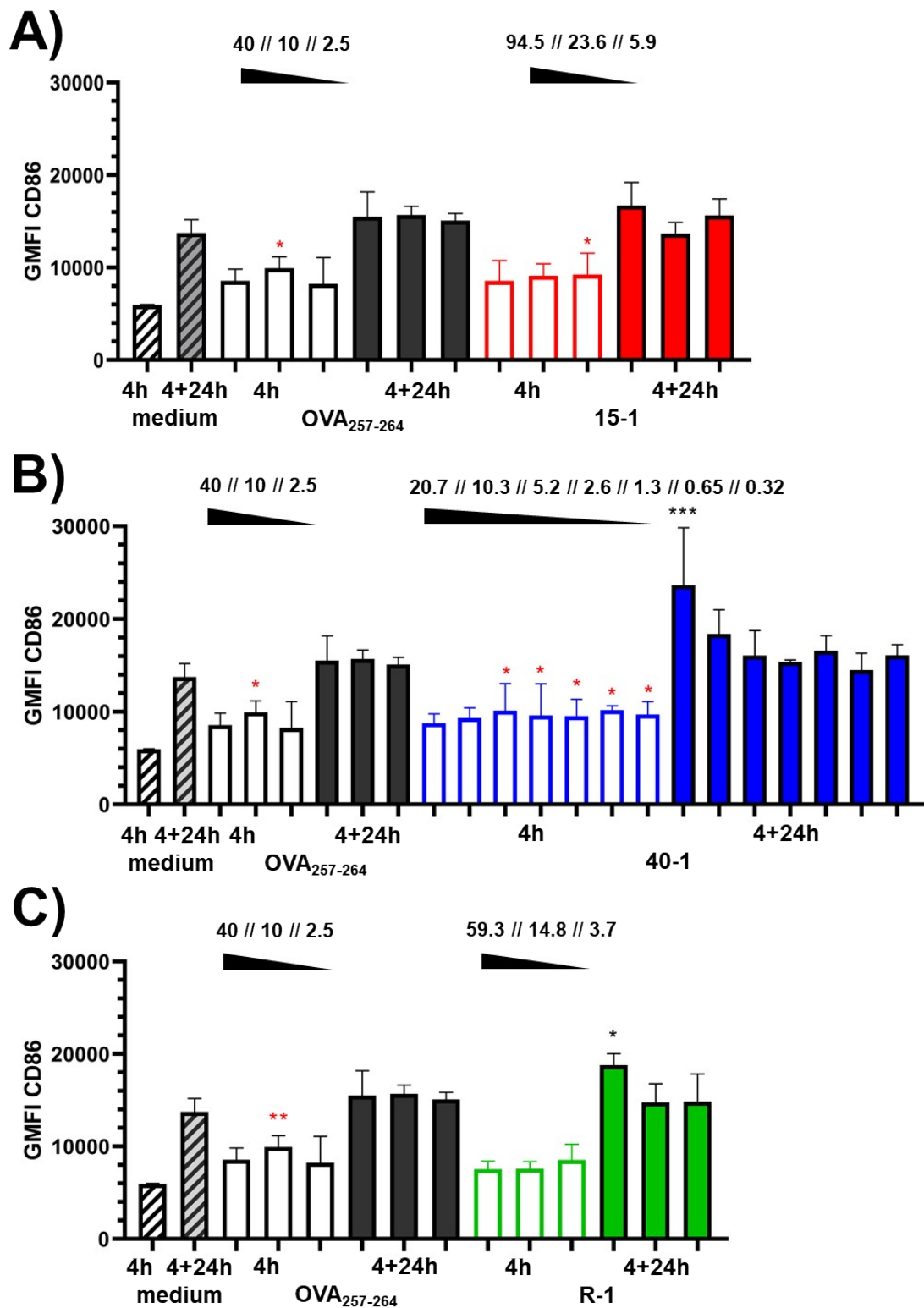


**Figure S15.** BMDCs activation was monitored through upregulation of CD86 cellular marker after a 4-hour incubation with GNPs and GNRs. Geometric mean fluorescence intensity (GMFI) gained for different samples was compared to the negative control (medium) and positive control (OVA<sub>257-264</sub>): (A) **15-1**, (B) **40-1**, and (C) **R-1**. Empty columns show data right after the 4-hour incubation, and solid columns – after 24 hours after the incubation. Epitope dosage per well (in ng/well) is shown above the indicator.

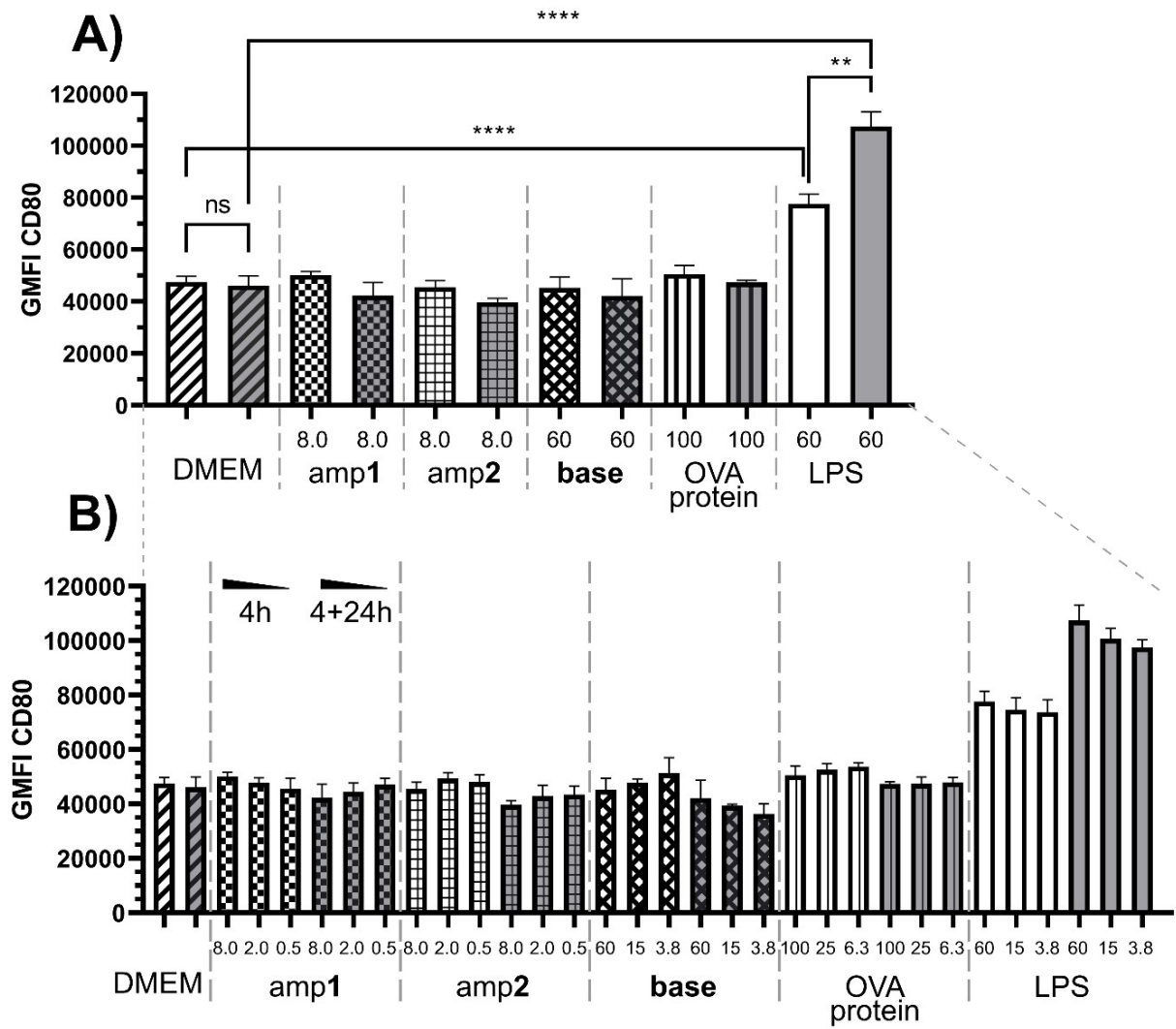


**Figure S16.** Geometric mean fluorescence intensity (GMFI) of CD80 signal gained for different control substances: three peptide amphiphiles (amp1, amp2, amp base), whole ovalbumin protein (OVA protein), bacterial lipopolysaccharides (LPS) were compared to the negative control (DMEM). Top concentrations comparable to the antigen loading of GNP and GNR at their top concentrations are shown (A) and the full concentration ranges are shown in (B). Empty columns show data right after the 4-hour incubation, and columns with a gray fill – 24 hours after the incubation. Dosage is given in µg/mL. Among all tested samples, only LPS showed statistically significant elevation in CD80 expression in comparison to DMEM control.



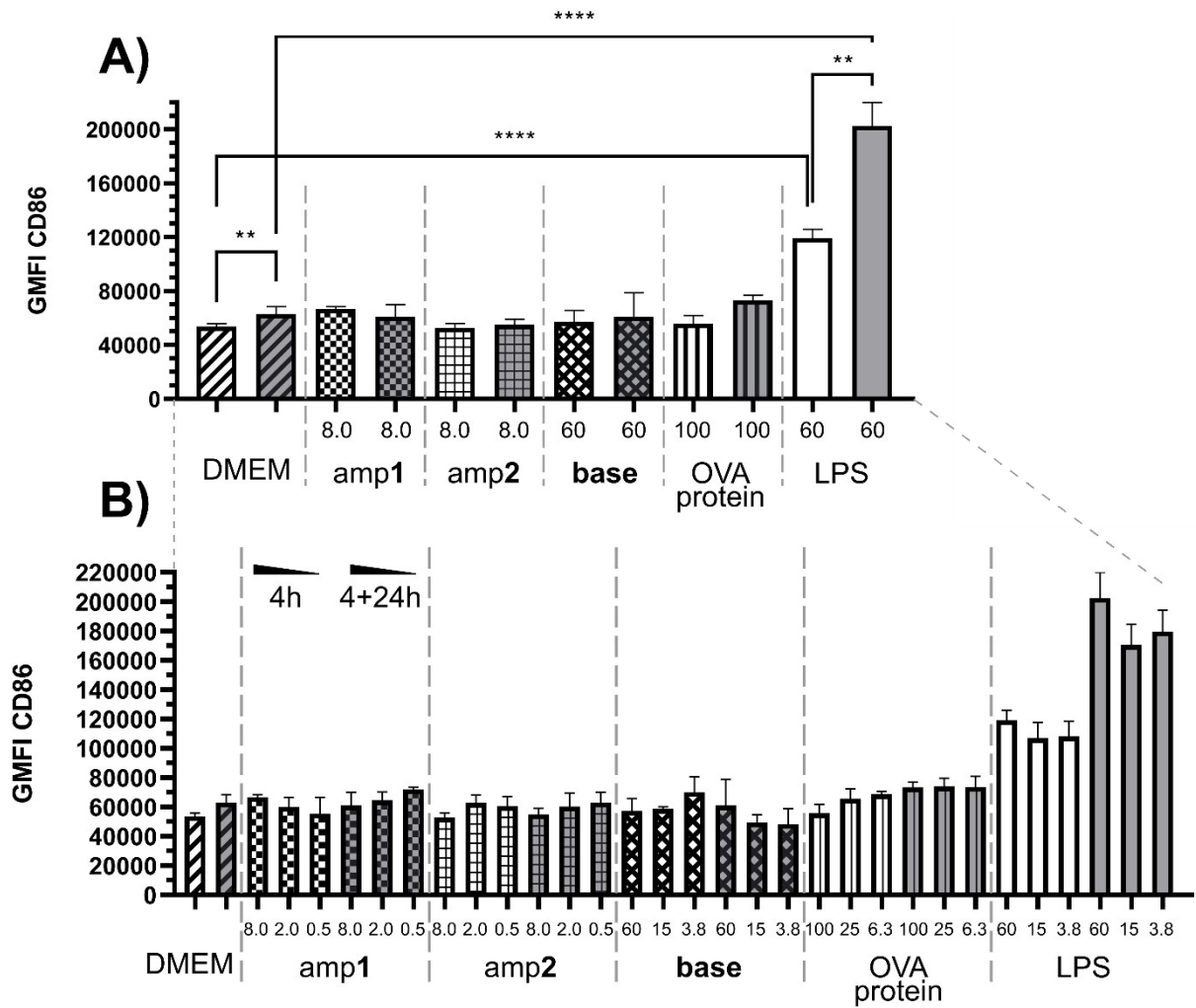


**Figure S17.** Geometric mean fluorescence intensity (GMFI) of CD86 signal gained for different control substances: three peptide amphiphiles (amp1, amp2, amp base), whole ovalbumin protein (OVA protein), bacterial lipopolysaccharides (LPS) were compared to the negative control (DMEM). Top concentrations comparable to the antigen loading of GNP and GNR at their top concentrations are shown (A) and the full concentration ranges are shown in (B). Empty columns show data right after the 4-hour incubation, and columns with a gray fill – 24 hours after the incubation. Dosage is given in µg/mL. Among all tested samples, only LPS showed statistically significant elevation in CD86 expression in comparison to DMEM control.

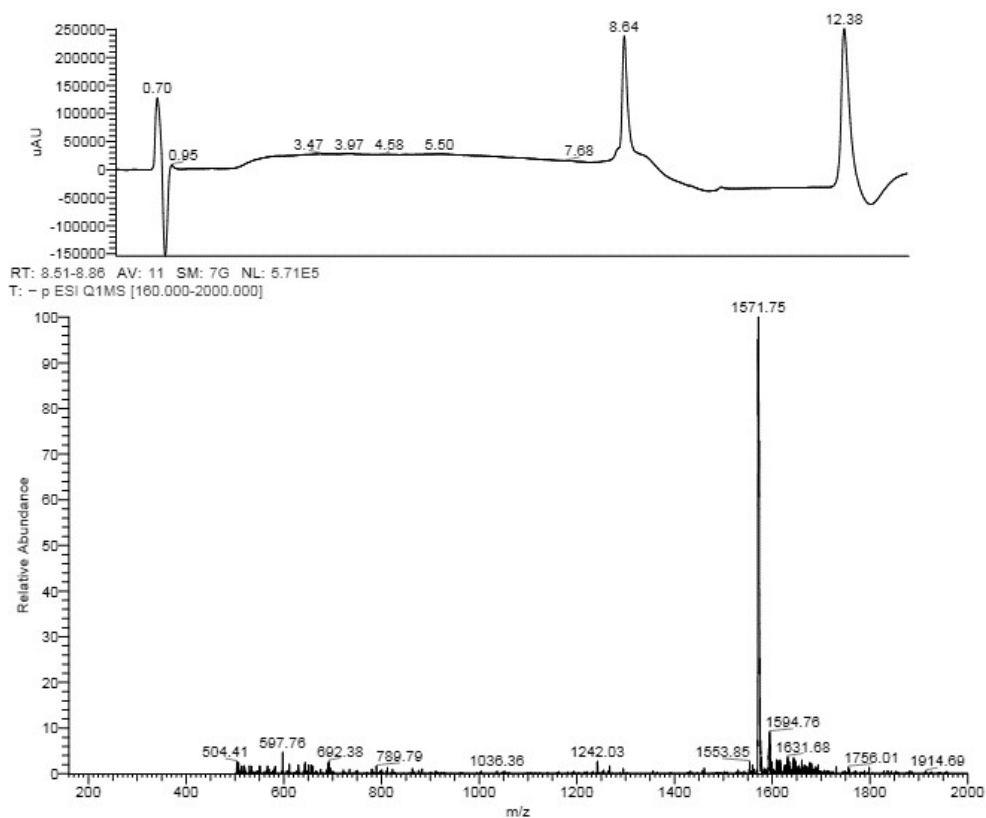


Figure S18. LC-MS spectrum for **base**.  $[M-H]^{-1}_{\text{theor}} = 1571.83$ .

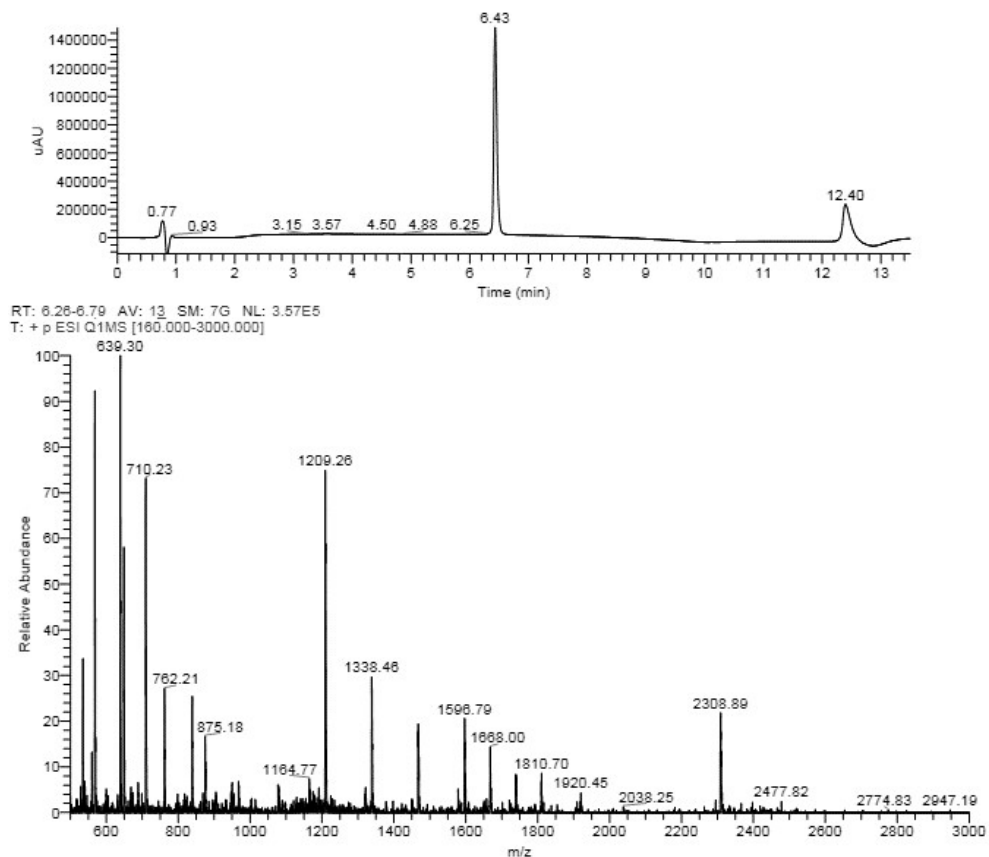
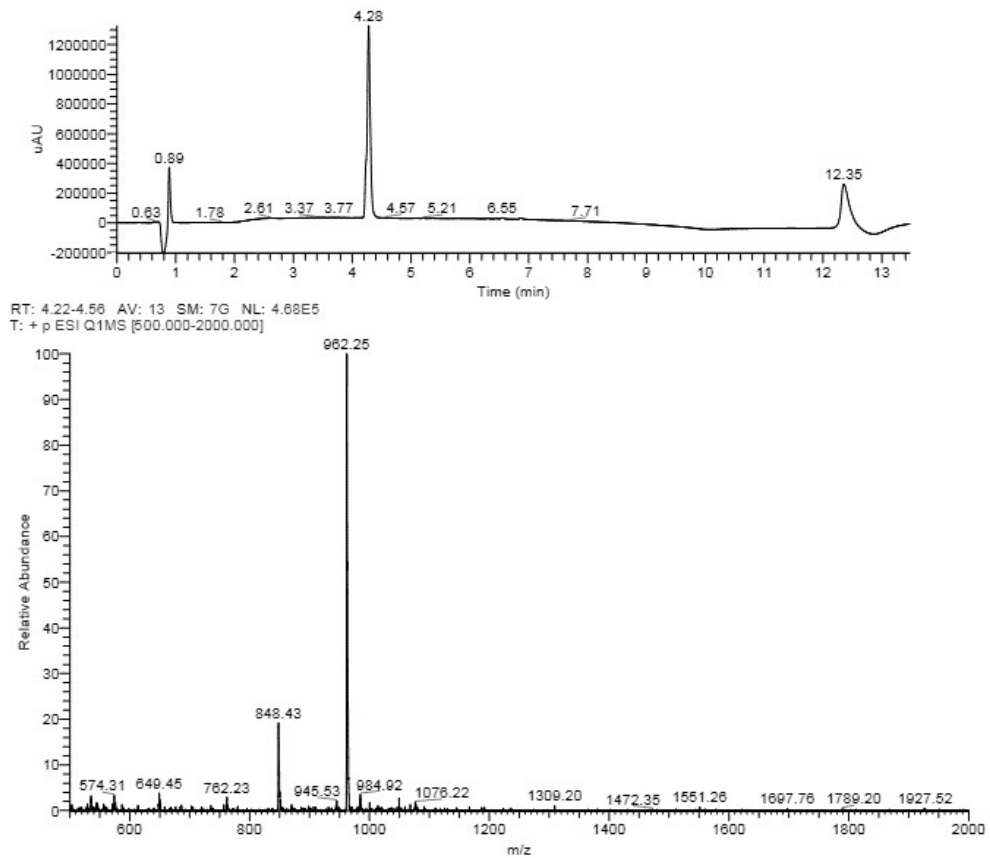
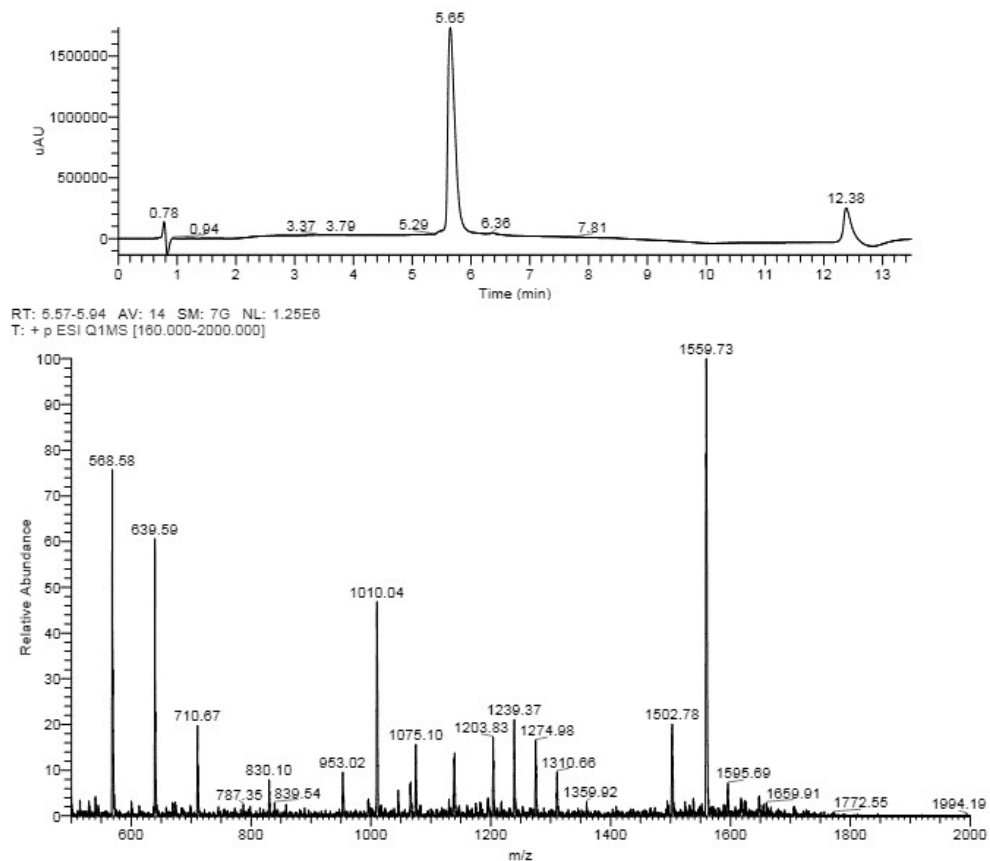


Figure S19. LC-MS spectrum for **1**.  $[M+H]^{+1}_{\text{theor}} = 2309.26$ .



**Figure S20.** LC-MS spectrum for OVA<sub>257-264</sub>.  $[M+H]^+$ <sub>theor</sub> = 962.54.  $[M+H]^+$  = 848.43 belongs to OVA<sub>257-264</sub> with a deletion of one isoleucine (I, Ile).



**Figure S21.** LC-MS spectrum for **2**.  $[M+2H]^{2+}$ <sub>theor</sub> = 1559.81.

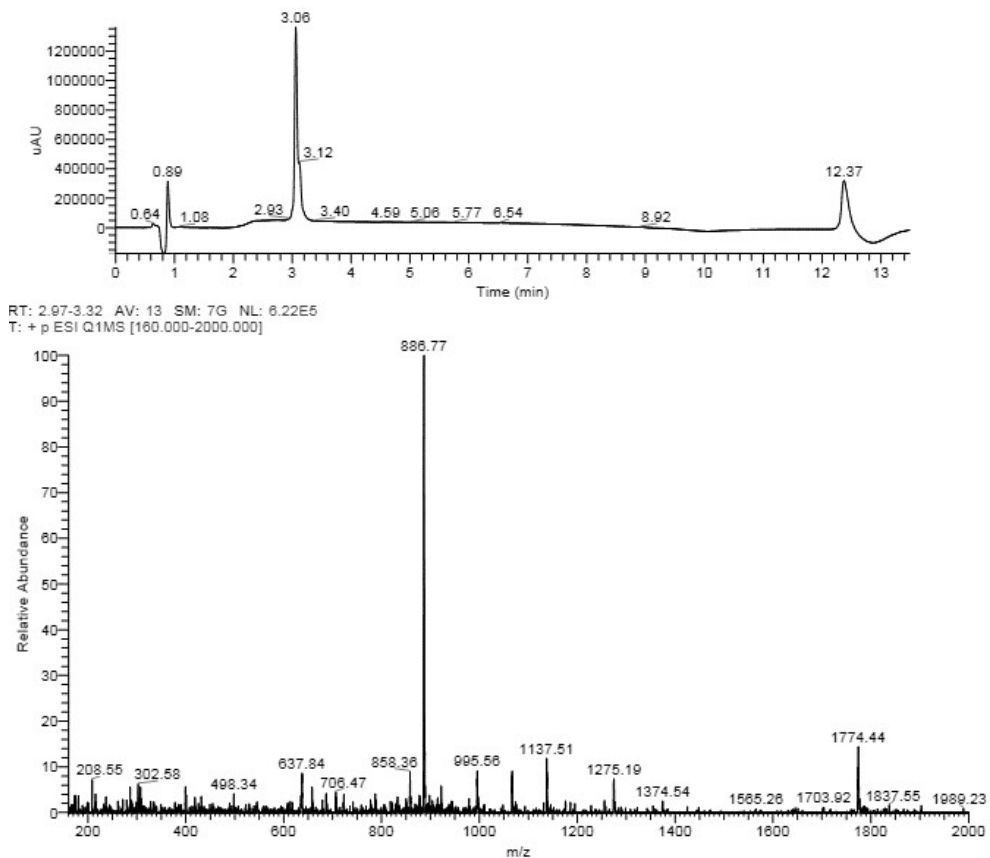


Figure S22. LC-MS spectrum for OVA<sub>323-339</sub>.  $[M+H]^+$ <sub>theor</sub> = 1773.90 and  $[M+2H]^2+$ <sub>theor</sub> = 887.45.

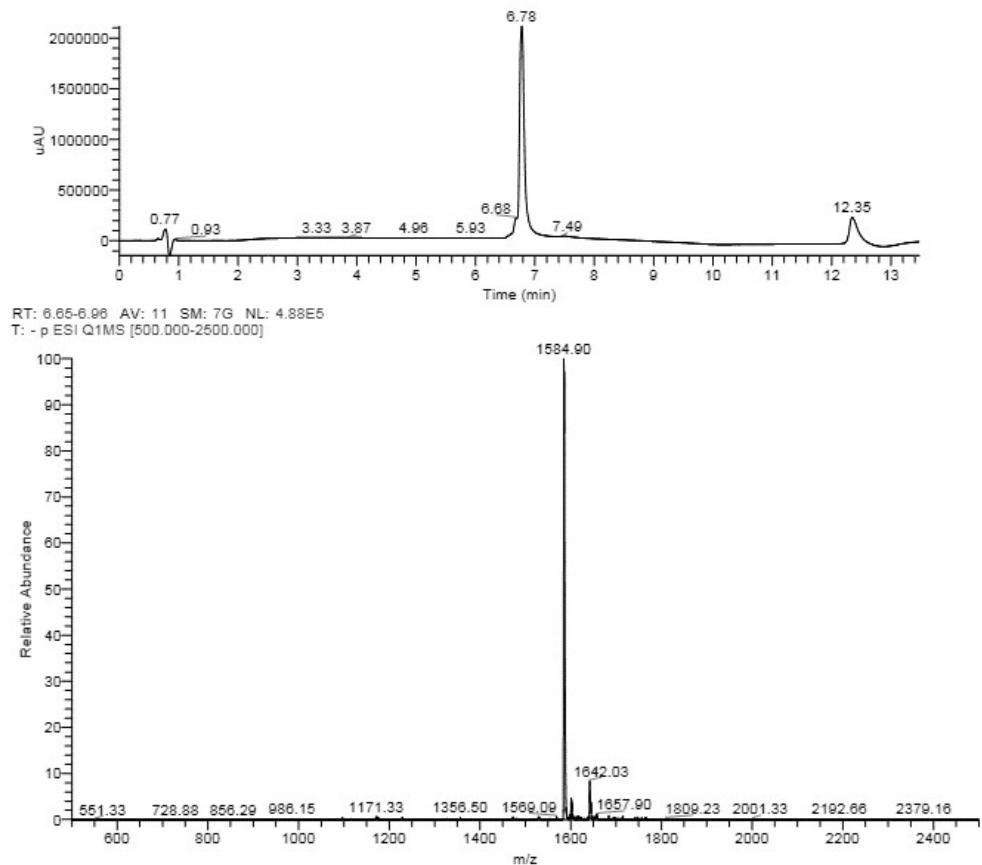


Figure S23. LC-MS spectrum for W.  $[M-H]^-$ <sub>theor</sub> = 1585.75.